Neutron-diffraction study of magnetically ordered $Er_2Fe_3Si_5$

A. R. Moodenbaugh and D. E. Cox
Physics Department, Brookhaven National Laboratory, Upton, New York 11973

C. B. Vining
Ames Laboratory—U.S. Department of Energy and Department of Physics, Iowa State University, Ames, Iowa 50011

C. U. Segre*
Physics Department, Rutgers University, Piscataway, New Jersey 08854
(Received 5 August 1983)

The magnetic ordering of $Er_2Fe_3Si_5$ has been studied by neutron-diffraction techniques at low temperatures. At 4.3 K, the crystal structure is tetragonal (space group $P4/mnc$, $a=10.393$ Å, $c=5.428$ Å). The atomic positional parameters were determined by Rietveld refinement of the data. Magnetic scattering peaks at positions incommensurate with the chemical cell are observed below 2.85 K. Below about 2.55 K, a second set of magnetic peaks appears, at positions commensurate with the chemical cell, but with the tetragonal a axis doubled. Between 2.55 and 2.45 K, the two sets of magnetic peaks coexist, and hysteresis of about 0.01 K is observed. In this temperature region, peaks from the incommensurate phase steadily decrease in intensity as temperature is reduced until, below 2.45 K, only commensurate peaks are present. The commensurate peaks increase in intensity as the temperature is reduced down to the lowest temperatures studied. Rietveld refinement of data taken at 1.83 K shows the magnetic intensities to be well accounted for by a noncollinear magnetic structure whose principal features are the following: (1) ordering occurs only at Er-atom sites, the moment being $8.2\mu_B$ at 1.83 K, and (2) the moments are ordered in the (001) planes with a noncollinear arrangement along the $\langle 110 \rangle$ set of directions, the c glide planes of the chemical structure being retained in the magnetic cell (space group C_pccm'). For the incommensurate model, all elements of the commensurate arrangement are retained, but a sinusoidal modulation along [001] with a wavelength of about $5.7c$ is introduced. This wavelength is independent of temperature to within ±3%. Specific-heat measurements were also performed on the sample. These measurements show three peaks, one at 2.75 K corresponding to the onset of magnetic order and two others at 2.45 and 2.43 K in the coexistence region of the incommensurate and commensurate phases.

INTRODUCTION

The relationship between magnetic behavior and superconductivity has been of longstanding interest. Recently, unusual superconducting and magnetic behavior in ternary rare-earth (RE) compounds has been discovered.[1] The coexistence of antiferromagnetic order and superconductivity has been extensively studied in the $M Mo_6S_8$ family[1] and, later, in the $M Rh_4B_4$ family.[2,3]

The tetragonal $M_2Fe_3Si_5$ compounds (prototype $Sc_2Fe_3Si_5$) initially attracted interest because, in spite of the high concentration of Fe, superconductivity was observed when the RE was nonmagnetic (Sc, Y, and Lu).[4–6] While most compounds in this family which contain a magnetic RE (i.e., Er) are not superconducting down to 1.2 K, many exhibit unusual magnetic behavior.

Magnetic susceptibility measurements provided the first evidence for antiferromagnetism in the $M_2Fe_3Si_5$ compounds.[4] Fe Mössbauer studies have shown that iron carries no moment in the compounds studied.[5–7] Gd Mössbauer results were interpreted to predict the presence of strong crystal electric fields (CEF's), and similar measurements on Er yielded a moment $\mu_{Er}=8.0\mu_B$.[8] Recently a series of heat-capacity measurements on $M_2Fe_3Si_5$ compounds at low temperatures was completed.[9,10] Peaks in the specific heat correspond well with Néel temperatures derived from susceptibility measurements. In several instances, including $Tb_2Fe_3Si_5$ and $Er_2Fe_3Si_5$, additional peak(s) were observed in the specific heat below T_N. Specific-heat data also suggest the importance of CEF effects.

In an earlier neutron-diffraction study of $Tb_2Fe_3Si_5$, two distinct magnetic structures were observed, one an incommensurate structure predominating from $T_N=10.3$ to 7 K, the other a commensurate structure below 7 K.[11] A specific-heat peak observed near 7 K corresponds well to the temperature region of the transformation between the two magnetic phases.[10,11] The present neutron-diffraction study of magnetic ordering in $Er_2Fe_3Si_5$ provides a second example of an incommensurate-commensurate transition in an antiferromagnetically ordered compound of the $M_2Fe_3Si_5$ family.

SAMPLE PREPARATION AND EXPERIMENTAL METHODS

Two samples of $Er_2Fe_3Si_5$, each of approximate mass 5 g, were prepared using identical methods. First, Fe and Si were arc-melted together, following which Er was melted into the alloy. About 0.5% of the total mass was lost in

the melting process for each sample. The ingots were heat treated in vacuum in a metal element furnace for two days at 1200 °C, two days at 1000 °C, and two days at 800 °C. About 0.2% of the mass was lost in this process, some due to spalling.

An x-ray-diffraction scan on a General Electric Company XRD-5 diffractometer equipped with a diffracted-beam monochromator, using Cu$K\alpha$ radiation, was performed on each sample with similar results. In each case there were several unidentified peaks due to impurity phases with intensities up to 3% of the intensity of the most intense peak in addition to peaks from $Er_2Fe_3Si_5$. Room-temperature lattice parameters were $a = 10.39 \pm 0.01$ Å and $c = 5.427 \pm 0.005$ Å.

Low-temperature heat-capacity measurements were performed on a solid fragment of one sample, B6-58, using the semiadiabatic calorimeter described previously.[9] Neutron-diffraction scans on the identical sample, now powdered, were performed below T_N. For the scan above $T_N = 2.85$ K, which was performed prior to the specific-heat measurements, portions of both samples were powdered and mixed together.

These scans were carried out at the Brookhaven National Laboratory High-Flux Beam Reactor. The neutron wavelength was 2.38 Å. A pyrolytic graphite monochromator and analyzer were set for the (002) reflection, higher-order contamination being suppressed with a graphite filter. Collimation was set at 20′, 40′, 40′, and 20′, respectively, for the in-pile, monochromator-sample, sample-analyzer, and analyzer-detector locations for the scan with the sample at 4.3 K. For the full scans at 2.57 and 1.83 K, the detector collimation was relaxed to 40′. Slightly different combinations were used for additional scans at various temperatures of selected peaks at low angles.

RESULTS

We will first describe the general nature of the results before analyzing them in terms of specific magnetic models. At 4.3 K, above T_N, the nuclear diffraction peaks are characteristic of $Er_2Fe_3Si_5$ (see Fig. 1, top panel). The lattice parameters are $a = 10.393$ Å and $c = 5.428$ Å, compared to those obtained at room temperature by x-ray diffraction, both in a previous study[4] ($a = 10.38$ Å and $c = 5.425$ Å) and in this work ($a = 10.39$ Å and $c = 5.427$ Å).

Below the ordering temperature $T_N = 2.85$ K, magnetic scattering peaks appear in the diffraction diagrams. These peaks, incommensurate with the chemical cell, are

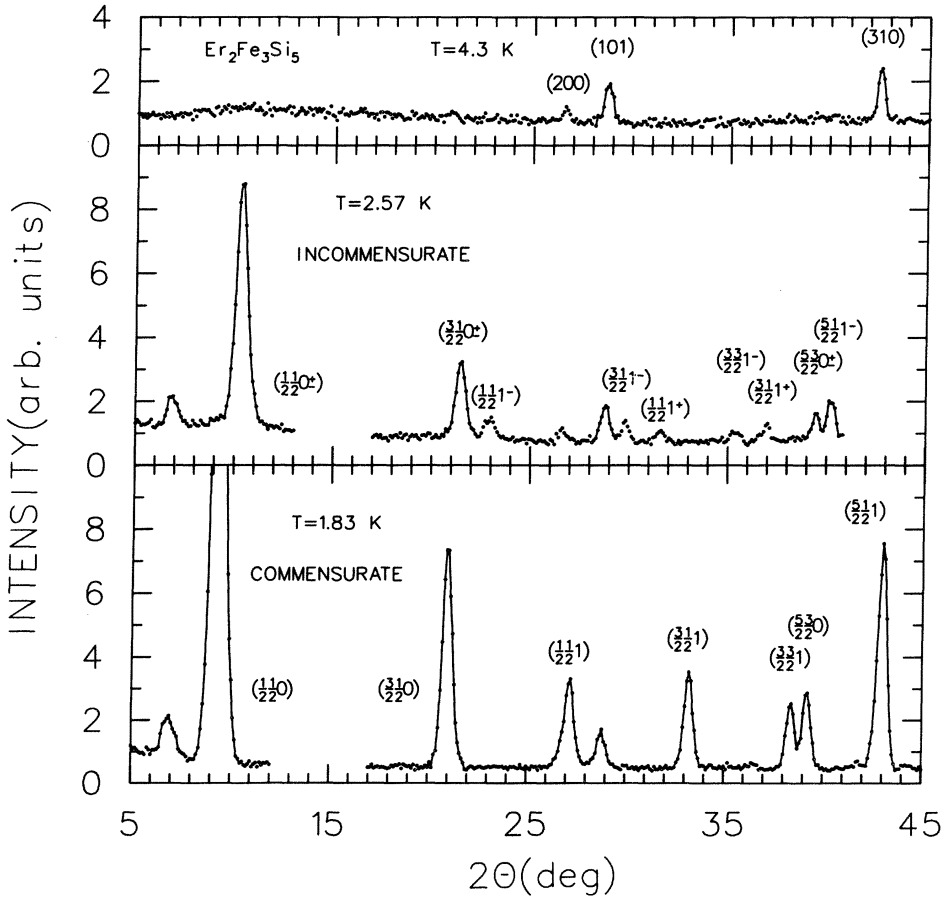

FIG. 1. Portions of neutron-diffraction scans of $Er_2Fe_3Si_5$ at three temperatures. Neutron wavelength is approximately 2.38 Å. Major nuclear peaks are identified for 4.3-K data. Major incommensurate and commensurate indexed magnetic peaks are identified in the two lower scans. In the 4.3-K scan an intensity of 1 corresponds to 100 counts; in the lower two scans an intensity of 1 corresponds to 200 counts. Commensurate $(\frac{1}{2}, \frac{1}{2}, 0)$ peak at $2\theta = 9.3°$ rises to $I = 30$ (corresponds to 6000 counts).

illustrated in the middle panel of Fig. 1 by a scan performed at 2.57 K. Below 2.55 K, a second set of magnetic peaks commensurate with the chemical cell appears. At the same time, the incommensurate set of peaks begins to decrease in intensity. The relative intensities of two representative peaks (the commensurate peak at $2\theta=9.3°$ and the incommensurate peak at $2\theta=10.3°$ in Fig. 1, bottom and middle panels, respectively) are plotted as a function of temperature in Fig. 2. Figure 1 (bottom) shows a full scan illustrating the diffraction pattern of the commensurate set of peaks, which can be indexed with tetragonal parameters ($2a$, c) with respect to the chemical cell. A notable feature is the existence of hysteresis in the region in which the two magnetic sets of peaks coexist (illustrated in Fig. 2), the hysteresis gap being about $T=0.01$ K. In addition to the above magnetic peaks, we observe one small peak (at $2\theta=6.9°$) which cannot be indexed with respect to either magnetic model. The peak appears near T_N, but its intensity increases monotonically down to 1.83 K in contrast to the behavior of the two principal sets of peaks.

The results of the heat-capacity measurements are shown in Fig. 3. They are essentially identical to those obtained for a sample of $Er_2Fe_3Si_5$ prepared independently with a slightly different annealing program.[10] A more detailed discussion is given in Ref. 10. The initial ordering temperature T_N is represented by a nearly logarithmic divergence in the heat capacity near 2.76 K. Near 2.45 K, a second, sharper transition is signalled by another anomaly in the heat capacity, which has two major features within a 20-mK region (see inset of Fig. 3). The sharpness and magnitude of this anomaly suggest a first-order magnetic transition, in agreement with the hysteresis noted in the neutron-diffraction measurements.

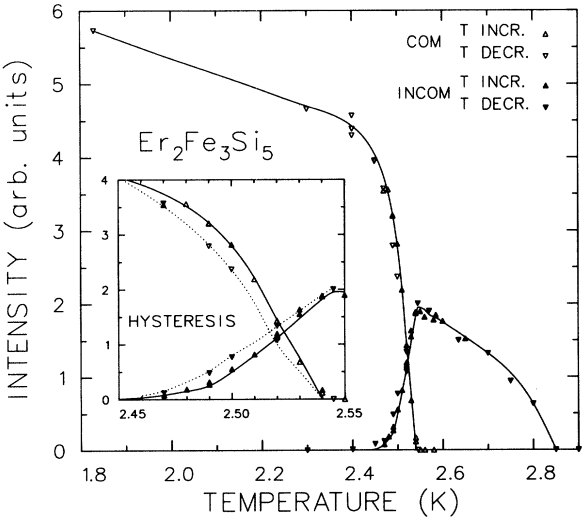

FIG. 2. Intensity as a function of temperature for two peaks, the $(\frac{1}{2},\frac{1}{2},0\pm)$ at $2\theta=10.3°$ representing the incommensurate phase (INCOM) and the $(\frac{1}{2},\frac{1}{2},0)$ at $2\theta=9.3°$ representing the commensurate (COM) phase. Different symbols are used for points taken after temperature was raised (T INCR.) or reduced (T DECR.) to demonstrate hysteresis (see the inset). Lines drawn are guides for the eye.

Rietveld refinement of the crystal structure at 4.3 K

The neutron-diffraction data for $Er_2Fe_3Si_5$ at 4.3 K were fit by refinement of the structure in the space group $P4/mnc$ using the Rietveld profile method.[12–14] For the refinement, atomic positions were initially assigned the values determined from a similar analysis for $Tb_2Fe_3Si_5$. Lattice parameters were assigned estimated values, and the overall temperature factor was set at zero. Regions of the scan which include scattering from the aluminum sample container were excluded from consideration. The background was determined by interpolation between values obtained from flat regions of the pattern between peaks. Neutron cross sections were taken from the compilation of Koester.[15] The results of the refinement are collected in Table I. The fit of the calculated curve to the data is shown in Fig. 4 together with the difference plot. The weighted profile reliability factor $R_{WP}=21.5\%$ can be compared with the expected, or statistical, $R_E=15.8\%$ (for definitions see Ref. 14). The overall temperature factor refines to a slightly negative value (only about 1 standard deviation from zero) and this does not significantly affect the positional parameters. In order to facilitate description of the magnetic structures, the positions of the Er atoms are shown projected on the (001) plane (Fig. 5). Er atoms are arranged in squares in this plane, two squares per chemical cell, each square approximately 3.63 Å on a side. One square is at $z=0$ (double circles in Fig. 5), and a second square is at $z=0.5c$ (open circles).

Magnetic scattering at 1.83 K

The results of analysis of the magnetic scattering at 1.83 K are described next. The peaks were indexed in terms of a tetragonal unit cell, with parameters ($2a$, c) with respect to the chemical cell. The fact that only half-integral magnetic indices are observed in the basal plane demands that a translation of one chemical cell length in either a-axis direction results in a reversal of sign of the

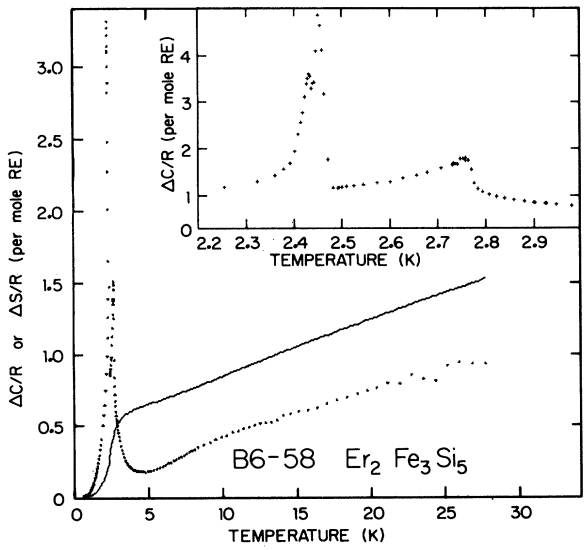

FIG. 3. Specific-heat capacity of $Er_2Fe_3Si_5$ at low temperatures. Note the expanded temperature scale of the inset.

TABLE I. Parameters from Rietveld refinements. U, V, and W are halfwidth parameters (Refs. 12 and 13). R_I, R_{WP}, and R_E are R factors defined by Hewat (Ref. 14) for integrated intensities, weighted profile, and statistical, or expected, values. Estimated standard deviations (ESD's) are given in parentheses based on the least significant figures. Values fixed initially have no ESD indicated. ESD's quoted for a and c do not take into account any uncertainty in the neutron wavelength.

Parameter	T=4.3 K	T=1.83 K
Er, 8(h)x	0.072(1)	0.071(1)
y	0.236(1)	0.240(1)
x	0	0
Fe_1, 8(h)x	0.377(1)	0.372(1)
y	0.358(1)	0.353(1)
z	0	0
Fe_2, 4(d)x	0	0
y	$\frac{1}{2}$	$\frac{1}{2}$
z	$\frac{1}{4}$	$\frac{1}{4}$
Si_1, 8(g)x	0.175(1)	0.169(3)
y	0.675(1)	0.669(3)
z	$\frac{1}{4}$	$\frac{1}{4}$
Si_2, 4(e)x	0	0
y	0	0
z	0.246(7)	0.270(6)
Si_3, 8(h)x	0.185(2)	0.171(3)
y	0.476(2)	0.473(1)
z	0	0
Er moment (μ_B)		8.2(1)
Overall temperature factor B (Å^2)	−0.5(4)	0
a (Å)	10.3930(5)	10.3583(12)
c (Å)	5.4277(5)	5.4074(6)
U (deg^2)	2.81(15)	2.22(13)
V (deg^2)	−2.86(19)	−1.97(9)
W (deg^2)	1.04(6)	0.66(13)
R_I (%)	8.4	4.2
R_{WP} (%)	21.5	11.6
R_E (%)	15.8	6.0

moment. Er atoms were assumed to be the only contributors to magnetic order, as suggested by Mössbauer measurements,[5–7] and found for Tb in the case of $Tb_2Fe_3Si_5$.[11]

Magnetic susceptibility results[6] and analysis of CEF's from Mössbauer measurements[8] indicate that ordering occurs with moments lying primarily within the (001) plane [in contrast to $Tb_2Fe_3Si_5$ (Ref. 11)], and this was borne out in the analysis of peak intensities. An important point in this analysis is the essentially zero contribution from the $(\frac{3}{2},\frac{3}{2},0)$ and $(\frac{5}{2},\frac{1}{2},0)$ reflections at $2\theta=28.5°$ and 34.3°, respectively (compare bottom with top scan in Fig. 2). Consideration of possible subgroups of $P4/mnc$ (Ref. 16) shows that no tetragonal magnetic lattice having the observed P-type centering[17] is compatible with these absences and other intensity data. A successful fit to the data was finally accomplished with a noncollinear model having the orthorhombic magnetic subgroup C_Pccm'. The c glide planes are retained and the Er moments are ordered in the tetragonal ⟨110⟩ set of directions within the basal plane, i.e., along the [100] and [010] directions of the orthorhombic cell. This orthorhombic cell has dimensions $a\sqrt{2}, a\sqrt{2}, c$ in terms of the chemical cell as shown in Fig. 5. Because the Er atoms are located on two sets of 8(l) sites with point symmetry m', the moments are required to lie in the basal plane. A number of other collinear and noncollinear models with various combinations of these symmetry elements were tried without success. For the Rietveld refinement initial values of the parameters were taken from the results of the 4.3-K refinement. Er moments were held equal with an initial value of $8\mu_B$ and directed along the ⟨110⟩ set of directions according to the model illustrated in Fig. 5. Atomic positions were restricted to the tetragonal symmetry of the chemical cell. Calculated spherical form factors for Er (Ref. 18) were used in the refinement of the data. In order to avoid correlation with the mag-

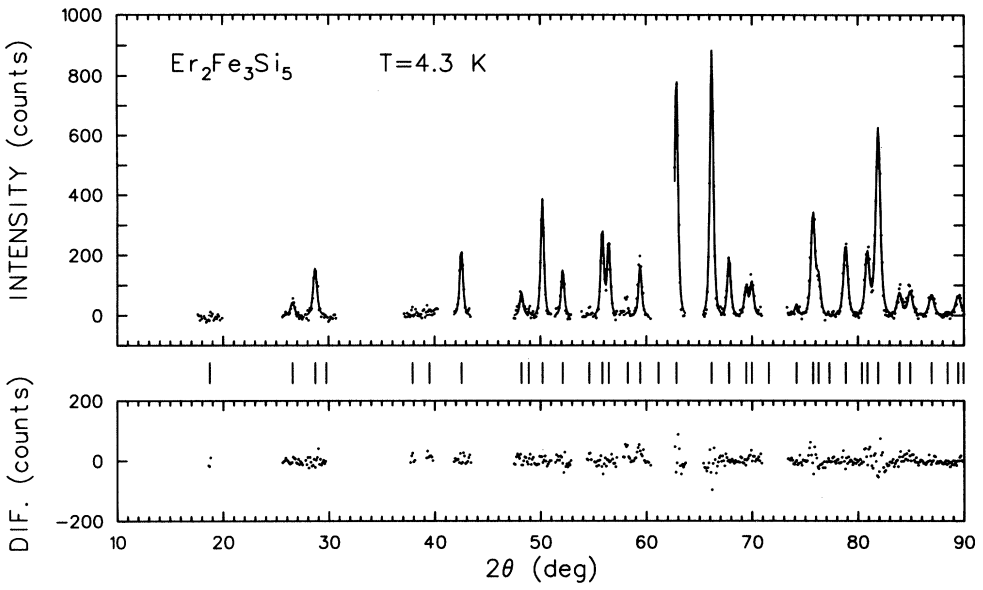

FIG. 4. Fit of Rietveld refinement results to 4.3-K data. Observed counts are data points. Calculated intensities are connected by the line. DIF is the difference between observed and calculated counts. Estimated background is subtracted from raw data before fitting and plotting. DIF is zero in excluded regions and in regions where no peak is predicted. Vertical marks between plots indicate predicted peak positions. Two regions of the pattern containing scattering from the Al sample holder were removed from consideration.

netic moment magnitude parameter which was otherwise observed, and on the basis of the 4.3-K results, the temperature factor was held at zero.

Results of the refinement in terms of the tetragonal chemical cell are shown in Table II, and the fit of the calculated curve to the data and the difference plot is shown in Fig. 6. The value determined for the Er magnetic moment, $8.2\mu_B$, agrees well with the results obtained in the analysis of the Mössbauer data.[8] The change of lattice parameters from 4.3 to 1.83 K is not believed to be significant since the 0.3% difference is within the uncertainty in the determination of the neutron wavelength.

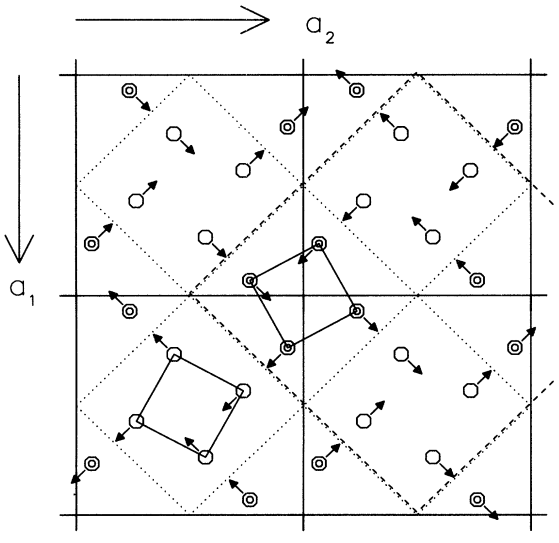

FIG. 5. Illustration of Er atomic positions in four adjacent chemical cells. View is along [001]. Cell edges are straight solid intersecting lines. Er atoms at $z=0$ are shaded symbols; Er atoms at $z=c/2$ are open symbols. Arrows represent moment directions. Dotted lines represent c glide planes. Dashed lines outline the orthorhombic magnetic cell.

Incommensurate magnetic scattering at 2.57 K

The incommensurate magnetic diffraction pattern is shown in Fig. 2 (middle). At 2.57 K the incommensurate magnetic peaks are near their maximum intensities and there is no scattering observed from the commensurate phase. The peak positions of the pattern can be accounted for on the basis of a sinusoidal modulation of the ordered moment amplitude along the [001] direction such that d^{*2} is given by

$$d^{*2}=[(h/2)^2+(k/2)^2]a^{*2}+(l\pm\delta)^2c^{*2}\,,$$

where $\delta=c/\lambda_i=0.176$, λ_i being the wavelength of the modulation (Table II).[19] As in the case of the commensurate pattern, the a axes are doubled, resulting in half-integral h and k values. For $l=0$ the value of d^{*2} differs from that of the corresponding commensurate magnetic peak by only second order in δ, as seen by comparing the positions of $(\frac{1}{2},\frac{1}{2},0\pm)$, $(\frac{3}{2},\frac{1}{2},0\pm)$, and $(\frac{5}{2},\frac{3}{2},0\pm)$ in Fig. 2 (middle) with the corresponding commensurate peaks in the bottom scan. For $l\neq 0$ the d-spacing equation is first order in δ, and two peaks—denoted $(h/2,k/2,l-)$ and $(h/2,k/2,l+)$—occur nearly symmetrically about the corresponding commensurate position. This can be seen by comparing the commensurate $(\frac{1}{2},\frac{1}{2},1)$ peak in Fig. 2 (bottom) with the $(\frac{1}{2},\frac{1}{2},1-)$ and $(\frac{1}{2},\frac{1}{2},1+)$ peaks in Fig. 2 (middle). A good fit to the observed intensities and positions is in fact obtained using the low-temperature model in Fig. 5 utilizing a moment of $7.2\mu_B$ with the simple addition of a modulation along [001] with $\delta=0.176$ (Table II).

TABLE II. Relative intensities and positions of incommensurate peaks at 2.57 K compared with calculated values based on model described in text. Er moment is $7.2\mu_B$.

$h\,k\,l$	I_c	I_0	$2\theta_c$ (deg)	$2\theta_0$ (deg)
$\frac{1}{2}\,\frac{1}{2}\,0\pm$	1.71	1.82	10.33	10.33
$\frac{1}{2}\,\frac{1}{2}\,0\pm$	0.49	0.51	21.42	21.45
$\frac{1}{2}\,\frac{1}{2}\,1-$	0.13	0.17	22.93	22.93
$\frac{3}{2}\,\frac{3}{2}\,0\pm$	0.00		28.58	
$\frac{3}{2}\,\frac{1}{2}\,1-$	0.13	0.12	29.76	29.79
$\frac{1}{2}\,\frac{1}{2}\,1+$	0.07	0.06	31.49	31.57
$\frac{5}{2}\,\frac{1}{2}\,0\pm$	0.00		34.38	
$\frac{3}{2}\,\frac{3}{2}\,1-$	0.09	0.06	35.38	35.35
$\frac{3}{2}\,\frac{1}{2}\,1+$	0.09	0.09	36.88	36.88
$\frac{5}{2}\,\frac{3}{2}\,0\pm$	0.17	0.12	39.43	39.45

There is no detectable variation in wavelength of the modulation $\lambda_i = c/\delta$ from about 2.5 to 2.8 K, to within the accuracy of measurement of the $(\frac{1}{2},\frac{1}{2},0\pm)$ peak position, typically $\pm 0.03°$ in 2θ based on a least-squares fit to a Gaussian peak shape. This results in an uncertainty in λ_i of at most $\pm 3\%$. This finding is in contrast to the $\approx 30\%$ variation of wavelength with temperature observed for the incommensurate modulation of $Tb_2Fe_3Si_5$.[10]

Temperature dependence of the Er moment

Figure 7 illustrates the temperature dependence of the Er moment, as calculated from the relative intensities of the $(\frac{1}{2},\frac{1}{2},0)$ or $(\frac{1}{2},\frac{1}{2},0\pm)$ peaks. The calculations are made using the $8.2\mu_B$ moment determined in the 1.83-K refinement for calibration on the basis of the models discussed in the preceding two sections. Omitted from the plot are values in the temperature region in which both structures exist (and in which there is hysteresis).

DISCUSSION

A noteworthy feature of the present work and the previous study of $Tb_2Fe_3Si_5$ (Ref. 11) is the overall similarity in magnetic behavior as a function of temperature. In both compounds only the RE moments contribute to magnetic order. In each case there is first a transition to an incommensurate phase modulated along the [001] axis, followed by a transition to a commensurate structure at a lower temperature. There is also an intermediate region in which incommensurate- and commensurate-type magnetic reflections are both present.

However, there are significant differences in the details of the behavior. In $Er_2Fe_3Si_5$ the two sets of reflections are present only over a temperature region of about 0.15 K, and there is a definite hysteresis in this region. This hysteresis, and the heat-capacity data,[10] suggest that this corresponds to a first-order transition and that two physically distinct phases are present in this region. This con-

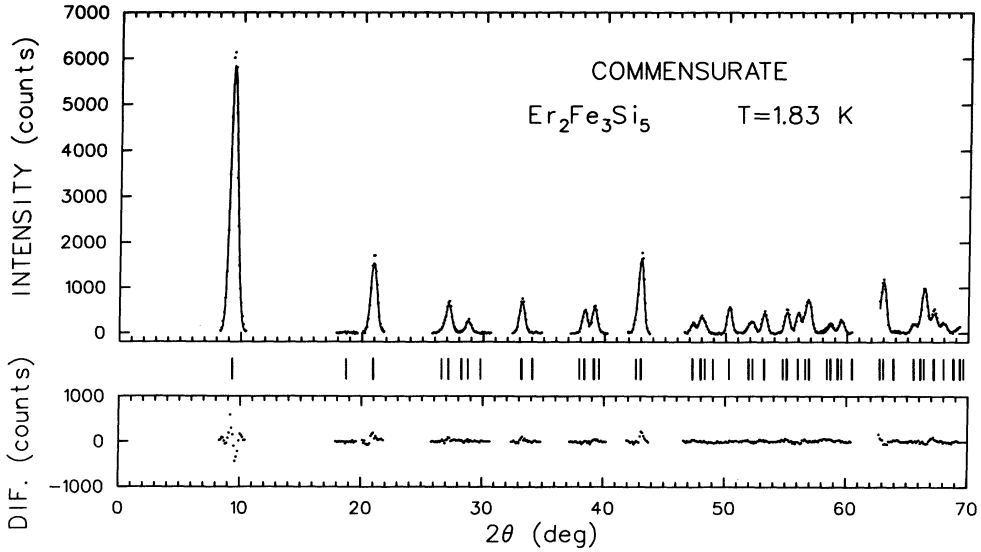

FIG. 6. Rietveld profile fit to 1.83-K data. Details of this plot are as described for Fig. 4.

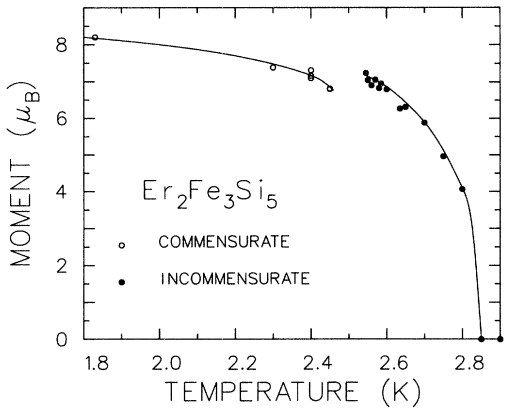

FIG. 7. Magnetic moment of Er as a function of temperature for incommensurate and commensurate models described in the text. Region in which two phases overlap and in which hysteresis occurs is excluded from consideration. The lines drawn are a guide for the eye.

trasts with the results for $Tb_2Fe_3Si_5$, where incommensurate and commensurate peaks were observed together over most of the temperature range between T_N at 10.3 K down to 4.55 K. No hysteresis was observed,[11] and the heat-capacity results[10] do not conclusively indicate a first-order transition. Thus this coexistence of patterns could correspond to a superposition of the Tb moments of the two models, which describes magnetic ordering throughout the material, rather than to two separate physical phases (as discussed in Ref. 11).

In $Er_2Fe_3Si_5$ the magnetic moments lie within the (001) planes. The most distinctive feature of the model (Fig. 5) is the parallel (or near parallel in the case of the incommensurate model) coupling of near-neighbor moments in adjacent (001) planes (separation distance of 3.91 Å). In $Tb_2Fe_3Si_5$ where the magnetic moments align along the (001) axis, the most noteworthy feature of the structure is the parallel coupling of nearest-neighbor moments within the (001) planes (separation of 3.61 Å).

ACKNOWLEDGMENTS

Work performed at Brookhaven National Laboratory is supported by the Division of Materials Sciences, U.S. Department of Energy, under Contract No. DE-AC02-76CH00016. Ames Laboratory is operated for U.S. Department of Energy by Iowa State University, under Contract No. W-7405-Eng-82. This research was supported by the Director for Energy Research, Office of Basic Sciences, under Contract No. WPAS-KC-02-02-02.

*Present address: Physics Department, Illinois Institute of Technology, Chicago, IL 60616.

[1]*Superconductivity in Ternary Compounds,* edited by Ø. Fischer and M. B. Maple (Springer, Berlin, 1982), Vols. I and II.

[2]H. B. Mackay, L. D. Woolf, M. B. Maple, and D. C. Johnston, J. Low Temp. Phys. 41, 639 (1980).

[3]H. R. Ott, L. D. Woolf, M. B. Maple, and D. C. Johnston, J. Low Temp. Phys. 39, 383 (1980).

[4]H. F. Braun, Phys. Lett. 75A, 386 (1980).

[5]J. D. Cashion, G. K. Shenoy, D. Niarchos, P. J. Viccaro, and C. M. Falco, Phys. Lett. 79A, 454 (1980).

[6]H. F. Braun, C. U. Segre, F. Acker, M. Rosenberg, S. Dey, and P. Deppe, J. Magn. Magn. Mater. 25, 117 (1981).

[7]J. D. Cashion, G. K. Shenoy, D. Niarchos, P. J. Viccaro, A. T. Aldred, and C. M. Falco, J. Appl. Phys. 52, 2180 (1981).

[8]D. R. Noakes, G. K. Shenoy, D. Niarchos, A. M. Umarji, and A. T. Aldred, Phys. Rev. B 27, 4317 (1983).

[9]C. B. Vining and R. N. Shelton, Phys. Rev. B 27, 2800 (1983).

[10]C. B. Vining and R. N. Shelton, Phys. Rev. B 28, 2732 (1983).

[11]A. R. Moodenbaugh, D. E. Cox, and H. F. Braun, Phys. Rev. B 25, 4702 (1982).

[12]H. M. Rietveld, Reactor Centrum Nederland Research Report No. RCN 104 (unpublished).

[13]H. M. Rietveld, J. Appl. Crystallogr. 2, 65 (1969).

[14]A. W. Hewat, Atomic Energy Authority Research Group Report No. RRL 73/897 (unpublished).

[15]L. Koester, in *Neutron Physics,* Vol. 80 of *Springer Tracts in Modern Physics,* edited by G. Hoehner (Springer, Berlin, 1977), Chap. 8.

[16]E. Ascher, Lattices of Equi-Translation Subgroups of the Space Groups, Internal Report, Battelle Institute, Geneva, 1968 (unpublished).

[17]W. Opechowski and R. Guccione, in *Magnetism VIIA,* edited by G. T. Rado and H. Suhl (Academic, New York, 1965).

[18]M. Blume, A. J. Freeman, and R. E. Watson, J. Chem. Phys. 37, 1245 (1962).

[19]G. E. Bacon, *Neutron Diffraction,* 3rd ed. (Clarendon, Oxford, 1975), Chap. 8.